Ocean Engineering 165 (2018) 277–292

Contents lists available at ScienceDirect

Ocean Engineering

journal homepage: www.elsevier.com/locate/oceaneng

Modelling of a tuned liquid multi-column damper. Application to floating wind turbine for improved robustness against wave incidence

Christophe Coudurier [b,*], Olivier Lepreux [a], Nicolas Petit [b]

[a] IFP Energies nouvelles, Rond-point de l'échangeur de Solaize, BP 3, 69360, Solaize, France
[b] MINES ParisTech, Centre Automatique et Systèmes, Unité Mathématiques et Systèmes, 60 Bd St-Michel, 75272, Paris, Cedex 06, France

ARTICLE INFO

Keywords:
Structural contol
U-tank
Anti-roll tank
U-tube
Tuned liquid column damper
Tuned liquid multi-column damper

ABSTRACT

In this paper, the coupling of a float with a tuned liquid multi-column damper (TLMCD), a novel structural damping device inspired by the classical tuned liquid column damper (TLCD), is modelled using Lagrangian mechanics. We detail the tuning of the design parameters for each considered variant of the TLMCD, and compare each of them against a layout of multiple TLCDs. The results show that the proposed TLMCD is superior to multiple TLCDs for this application as it is more robust against wave incidence and it creates significantly less parasitic oscillations.

1. Introduction

Wind power is the second fastest growing source of renewable electricity (National Renewable Energy Laboratory, 2012) in terms of installed power. The construction of offshore wind farms is growing worldwide. In Europe, offshore wind energy is expected to grow to 23.5 GW by 2020, tripling the installed capacity in 2015 (Ernst and Young, 2015). The major causes of this recent trend are the strength and regularity of wind far from the shore, which should allow for the easy mass production of electricity. To generate offshore wind energy, two types of technologies have been considered: fixed-bottom wind turbines (foundations fixed into the seabed) and floating wind turbines (FWTs). The fixed-bottom offshore wind turbine technology is too costly for use in water deeper than 60 m (Musial et al., 2006). This disqualifies them from use in most seas. FWTs are a tempting alternative. One advantage is that FWTs are not as dependent on seabed conditions for installation and can be moved to a harbour for maintenance. The main drawback of FWTs is their sensitivity to surrounding water waves that increase the mechanical load on the wind turbine (Jonkman, 2007), hence reducing the lifespan of its mechanical parts. This sensitivity can be mitigated by increasing the mass and size of the mechanical structure. However, this leads to a prohibitive rise in the cost per kWh.

Previous studies have proposed compensating for tower fore-aft oscillations using collective and individual blade pitch control to modify the wind thrust forces (Jonkman, 2007; Namik, 2012; Christiansen et al., 2013). This solution has the advantage of requiring no structural modification, but delivers limited performance. The tower movements are still many times superior to those observed on onshore wind turbines. Instead of using aerodynamic forces, it is tempting to consider using hydrodynamic forces. In naval engineering, considerable attention has been paid to ship roll damping (since the advent of steamboats). However, most solutions involve the use of the speed of the ship relative to the water to generate lift to control the roll (Perez and Blanke, 2012) and, for this reason, are not easily transferable to our problem.

In addition to naval engineering, civil engineering has been a great contributor to such approaches, as skyscrapers are highly sensitive to wind gusts and earthquakes. This general field (*structural control*) is beyond the scope of this paper, and the reader can refer to (Saeed et al., 2013) for an overview. To improve the response of massive structures to external disturbances, attached moving masses, such as tuned mass dampers (TMD), can be employed. Among the most economical and efficient solutions is the tuned liquid column damper (TLCD), also known as the anti-roll tank or the U-tank. As originally proposed by Frahm (Frahm, 1911; Moaleji and Greig, 2007) to limit ship roll, it is a U-shaped tube on a plane orthogonal to the ship's roll axis, and is generally filled with water. The liquid inside the TLCD oscillates due to the movement of the structure and liquid's energy is dissipated through a restriction located in the horizontal section. The TLCD is usually chosen to damp the natural frequency of the structure. While TLCD systems have been modelled in the past by, for instance, (Chang and Hsu, 1998; Gao et al., 1997), it remains an active field of research (Di Matteo et al., 2014). A considerable amount of relevant research has been conducted over the

* Corresponding author.
E-mail addresses: christophe.coudurier@mines-paristech.fr (C. Coudurier), olivier.lepreux@ifpen.fr (O. Lepreux), nicolas.petit@mines-paristech.fr (N. Petit).

https://doi.org/10.1016/j.oceaneng.2018.03.033
Received 22 August 2017; Received in revised form 7 March 2018; Accepted 11 March 2018
Available online 25 July 2018

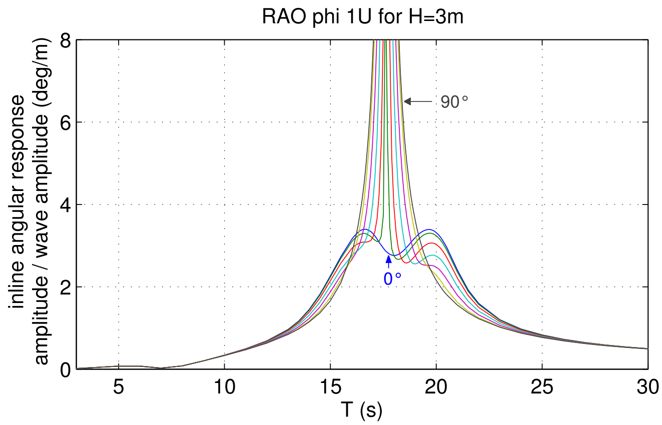

Fig. 1. RAO of the float damped by a single TLCD for different incident angles.

last two decades on civil engineering applications, where most of the work has focused on determining the optimal design of passive TLCDs, such as (Gao et al., 1997; Wu et al., 2009; Yalla and Kareem, 2000).

Several studies have shown that the structural control of floating wind turbines using active (Lackner and Rotea, 2011; Namik et al., 2013) or passive (Stewart and Lackner, 2013; Si et al., 2014) TMDs can substantially reduce the load on the wind turbine. Other studies (Coudurier et al., 2015; Luo et al., 2011; Shadman and Akbarpour, 2012) have shown that the passive and semi-active TLCDs are an interesting alternative.

In this paper, we consider the damping of an offshore platform subject to waves of various angles of incidence. Such a system behaves as a six-DOF periodically oscillating rigid body. We try to minimize the roll and pitch oscillations by means of a TLCD, and neglect aerodynamic forces. Due to the mooring system, we cannot easily change the orientation of the float to adapt to the wave incidence. In the past, we studied the disturbance rejection capabilities of a TLCD aligned with the wave incidence (Coudurier et al., 2015). As shown in Fig. 1, the damping provided by the TLCD is not robust against a change in the wave incidence.

This work is partly based on (Holden and Fossen, 2012). However, unlike the ships considered there, the float we consider has isotropic properties, meaning that its roll and pitch motions have the same characteristics. Here we go a step further introducing three multidirectional damping devices based on the concept of the TLCD. Their dynamics and their robustness against wave incidence are investigated.

2. Description of the system

The floater considered was the MIT/NREL Shallow Drafted Barge and the wind turbine was an NREL 5 MW; both are described in Tables 2 and 3.

Table 1
Nomenclature.

$\mathscr{R}_n$	Earth-fixed frame
$\mathscr{R}_b$	Barge-fixed frame
$R(\Theta) \in \mathbb{R}^{3\times3}$	Rotation matrix from $\mathscr{R}_b$ to $\mathscr{R}_n$ so that $\forall r \in \mathbb{R}^3$, $r^n = Rr^b$
$x^n = [x, y, z]^\top \in \mathbb{R}^3$	Position of the centre of gravity of barge in $\mathscr{R}_n$
$\Theta = [\varphi, \theta, \psi]^\top \in \mathbb{R}^3$	Euler triple associated with R
$\nu^b \in \mathbb{R}^3$	Speed of CoG, the centre of gravity of the float
$\omega^b \in \mathbb{R}^3$	Rotational speed of $\mathscr{R}_b$ with respect to $\mathscr{R}_n$
nc	Number of variables needed to describe the liquid speed in the TLCD/TLMCD
$w \in \mathbb{R}^{nc}$	Vector describing the position of the liquid in the TLMCD
$w_i \in \mathbb{R}$	position of the liquid in the i^{th} element
$q = [x^{n\top}, \Theta^\top, w^\top]^\top \in \mathbb{R}^{6+nc}$	System's generalized positions
$\nu = [\nu^{n\top}, \omega^{b\top}, \dot{w}^\top]^\top \in \mathbb{R}^{6+nc}$	System's speeds
$G(\Theta) \in \mathbb{R}^{3\times3}$	Matrix relating $\dot\Theta$ and ω^b so that $\omega^b = G\dot\Theta$

(continued on next column)

Table 1 (*continued*)

$\mathscr{P}(\Theta) \in \mathbb{R}^{6+nc\times6+nc}$	Matrix relating $\dot q$ and ν so that $\nu = \mathscr{P}\dot q$
$S(\cdot) \in \mathbb{R}^{3\times3}$	Skew symmetric matrix representing the
$S^2(\cdot) = S(\cdot)^\top S(\cdot)$	cross-product in $\mathbb{R}^3$, with $S(x)y = x \times y$.
A_v and $A_h \in \mathbb{R}$	Cross-sections of the vertical and horizontal tubes of the tank
$\nu \in \mathbb{R}$	Cross-section ratio defined as $\nu \triangleq \frac{A_v}{A_h}$
$\sigma_i \in \mathbb{R}$	Curvilinear abscissa describing the geometry of the i^{th} element
$\varsigma_i, \varsigma_{pi}, \varsigma_{si} \in \mathbb{R}$	Abscissa of the free surfaces in the i^{th} element
$\alpha_i \in \mathbb{R}$	orientation angle of the i^{th} element
$r^b(\sigma) = [x_t^b, y_t^b(\sigma), z_t^b(\sigma)]^\top \in \mathbb{R}^3$	Function describing the centreline of the damper
$A(\sigma) > 0 \in \mathbb{R}$	Cross-section of the tank at abscissa σ
L_v and $L_h \in \mathbb{R}$	Length of the vertical and horizontal tubes of the TLCD
$e \in \mathbb{R}$	Distance between CoG and the horizontal tubes
$\rho \in \mathbb{R}$	Liquid density
$\eta \in \mathbb{R}^{nc}$	Vector of the head-loss coefficients of the restrictions
$M_s = M_s^\top \in \mathbb{R}^{6\times6}$	Mass matrix of the float
$m_t \in \mathbb{R}$	Total mass of the liquid in the damping system
$Q_{hydro} \in \mathbb{R}^6$	Generalized force due to the barge/waves interactions
$Q_{res} \in \mathbb{R}^{nc}$	Generalized force due to the restrictions in the TLMCD
$F_h \in \mathbb{R}^N$	Force generated by the fluid flow through the restrictions
$\beta \in \mathbb{R}$	Wave incidence angle

The barge and the wind turbine are modelled as a single rigid body, referred to as “the float” in this paper. Deformations in the wind turbine are neglected as its resonant period is inferior to the period of the monochromatic waves we consider here – ranging from 3 s to 30 s. The float is studied with all six degrees of freedom. To avoid any bias in the study, we do not consider the interaction between the rotor and the wind because the damping induced is dependent on the controller chosen for

Table 2
Summary of MIT/NREL barge properties, from (Jonkman, 2007).

Diameter, Height	36 m, 9.5 m
Draft, Freeboard	5 m, 4.5 m
Water Displacement	5089 m^3
Mass, Including Ballast	4,519,150 kg
CM Location below SWL	3.88238 m
Roll Inertia about CM	390,147,000 kg m^2
Pitch Inertia about CM	390,147,000 kg m^2
Yaw Inertia about CM	750,866,000 kg m^2
Anchor (Water) Depth	200 m
Separation between Opposing Anchors	436 m
Unstretched Line Length	279.3 m
Neutral Line Length Resting on Seabed	0 m
Line Diameter	0.127 m
Line Mass Density	116 kg/m
Line Extensional Stiffness	1,500,000,000 N

Table 3
Gross properties chosen for the NREL 5-MW baseline wind turbine, from (Jonkman, 2007).

Rating	5 MW
Rotor Orientation, Configuration	Upwind, 3 Blades
Control Variable Speed	Collective Pitch
Drivetrain High Speed	Multiple-Stage Gearbox
Rotor, Hub Diameter	126 m, 3 m
Hub Height	90 m
Cut-In, Rated, Cut-Out Wind Speed	3 m/s, 11.4 m/s, 25 m/s
Cut-In, Rated Rotor Speed	6.9 rpm, 12.1 rpm
Rated Tip Speed	80 m/s
Overhang, Shaft Tilt, Precone	5 m, 5° , 2.5°
Rotor Mass	110,000 kg
Nacelle Mass	240,000 kg
Tower Mass	347,460 kg
Coordinate Location of Overall CM	(-0.2 m, 0.0 m, 64.0 m)

the wind turbine (its impact can be negative or positive (Larsen and Hanson, 2007)). An illustration of the float with a 3S TLMCD is given in Fig. 2.

2.1. Assumptions

To model the dynamics of the tank, we make the following assumptions:

1. the float is rigid. Therefore,
2. its centre of gravity, CoG, is immobile in the frame fixed to the barge,
3. the liquid in the TLCD is incompressible,
4. the column width is small with respect to length,
5. the flow of liquid in the tank is uniform in each column,
6. the position of the free surface of liquid in the tank is within the vertical column (i.e. vertical columns are never empty).

2.2. Kinematics of the tank

A TLCD is composed of two vertical tanks of cross-section A_v connected by a horizontal duct of cross-section A_h. Liquid flows from one vertical column to the other through the horizontal tube. The restriction causing the damping (head loss) is located in the middle of the horizontal part. Fig. 3 is an illustration of the TLCD with the parameters presented in this subsection.

As we neglect the width of the columns, the TLCD geometry is defined by a line whose coordinates are expressed in the frame fixed to the barge

$$r^b(\sigma) \triangleq \left[x_t^b, y_t^b(\sigma), z_t^b(\sigma)\right]^\top$$

with

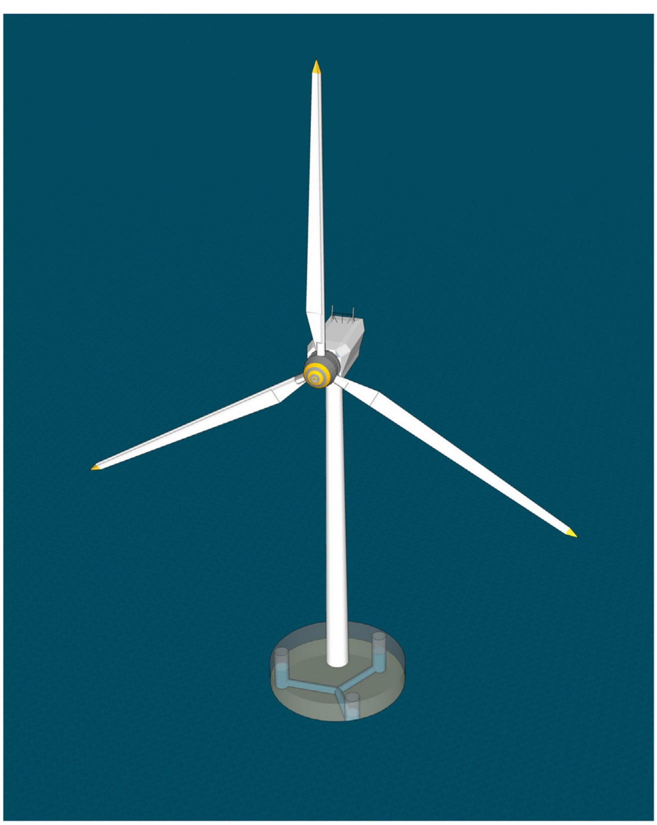

Fig. 2. Illustration of the float with a 3S TLMCD.

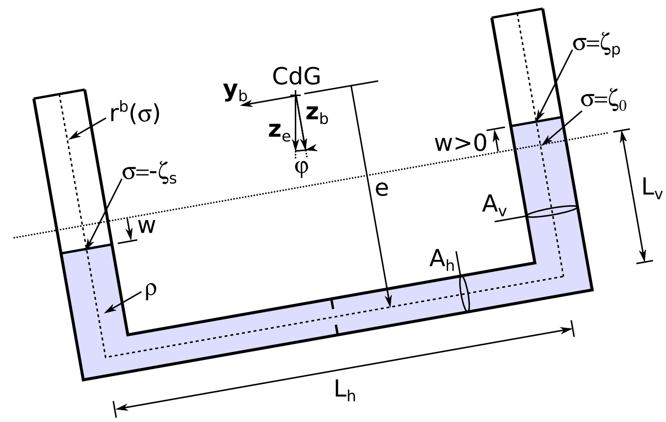

Fig. 3. Scheme of a single TLCD illustrating the main variables.

$$y_t^b(\sigma) \triangleq \begin{cases} \frac{L_h}{2} & \sigma \le -\frac{L_h}{2} \\ -\sigma & -\frac{L_h}{2} < \sigma \le \frac{L_h}{2} \\ -\frac{L_h}{2} & \frac{L_h}{2} < \sigma \end{cases} \quad z_t^b(\sigma) \triangleq \begin{cases} e + \frac{L_h}{2} + \sigma & \sigma \le -\frac{L_h}{2} \\ e & -\frac{L_h}{2} < \sigma \le \frac{L_h}{2} \\ e + \frac{L_h}{2} - \sigma & \frac{L_h}{2} < \sigma \end{cases}$$

where x_t^b is defined for each damping system to generate a symmetric problem, and where σ is the curvilinear abscissa along the geometry of the tank ($\sigma = 0$ is at the centre of the horizontal tube, and for $\sigma > 0$ $y_t^b(\sigma)$ is negative). We write $\frac{\mathrm{d}r^b}{\mathrm{d}\sigma}(\sigma)$ as the unit vector tangent to the tank.

We define the cross-sectional area of the tank as

$$A(\sigma) \triangleq \begin{cases} A_v & \sigma \le -\frac{L_h}{2} \\ A_h & -\frac{L_h}{2} < \sigma \le \frac{L_h}{2} \\ A_v & \frac{L_h}{2} < \sigma \end{cases}$$

In this paper, the damping systems we consider consist of N identical elementary subsystems (referred to as elements), which are regularly rotated around $(CoG, \mathbf{z}_b)$. The geometry of each element is given by $R_z(\alpha_i) r^b(\sigma_i)$ where

$$R_z(\alpha_i) = \begin{bmatrix} \cos(\alpha_i) & -\sin(\alpha_i) & 0 \\ \sin(\alpha_i) & \cos(\alpha_i) & 0 \\ 0 & 0 & 1 \end{bmatrix}$$

is the rotation matrix around $\mathbf{z}$ and where α_i is the orientation angle of the i^{th} element. Let $v_i(\sigma_i)$ be the algebraic speed in the i^{th} element of the damping system. By convention, $v_i(\sigma_i)$ is positive if the liquid flows towards positive σ. The vector $\mathbf{v}_i^b(\sigma_i)$ is the speed of the liquid in the i^{th} element expressed in $\mathscr{R}_b$ as

$$\mathbf{v}_i^b(\sigma_i) = v_i(\sigma_i) R_z(\alpha_i) \frac{\mathrm{d}\mathbf{r}^b}{\mathrm{d}\sigma}(\sigma_i) \tag{1}$$

We also introduce $\mathscr{V}_h$, the vector of algebraic speeds in the horizontal tubes, as

$$\mathscr{V}_h \triangleq \begin{bmatrix} v_1(0) \\ \vdots \\ v_N(0) \end{bmatrix} \qquad \mathscr{V}_h = P_h \dot{w} \tag{2}$$

with P_h given for each damping system in the Appendices.

3. Linearised dynamics

We define $X \triangleq [\mathbf{x}^n \quad \Theta \quad w \quad \dot{\mathbf{x}}^n \quad \dot{\Theta} \quad \dot{w}]^\top$ the state vector of our system, with $x^n = [x, y, z]^\top \in \mathbb{R}^3$ the position of the systems centre of gravity, $\Theta = [\varphi, \theta, \psi]^\top \in \mathbb{R}^3$ the orientation of the float, $w \in \mathbb{R}^{nc}$ and nc the number of variables describing the speed of the liquid inside the TLCD (nc will be detailed in §4 for each variant). The linearised model writes

$$\dot{X} = \mathscr{A}(\omega)X + \mathscr{B}(\omega)\begin{bmatrix} F_{hydro}(\omega, H) \\ Q_{res}(\eta) \end{bmatrix}$$

with

$$\mathscr{A}(\omega) = \begin{bmatrix} 0_{6+nc\times 6+nc} & \mathrm{I}_{6+nc\times 6+nc} \\ (M(0)+A(\omega))^{-1}K & (M(0)+A(\omega))^{-1}(C(0,0)+B(\omega)) \end{bmatrix}$$

$$\mathscr{B}(\omega) = \begin{bmatrix} 0_{6+nc\times 6+nc} \\ (M(0)+A(\omega))^{-1} \end{bmatrix}$$

where $M(0)$ and $C(0,0)$ the mass matrices given in §4 where $(q, \dot{q}) = 0$. The matrices $A(\omega)$ and $B(\omega)$ are respectively the radiation added mass and damping matrices, with ω the angular frequency of the monochromatic wave. The stiffness matrix K accounts for buoyancy and gravity. The forces applied on the float and the liquid inside the TLCD are $F_{hydro}(\omega, H)$, depending on the angular frequency ω and H the wave height, and $Q_{res}(\eta)$ as given in §4.2.

This linear model is based on the non-linear model presented in §4, which can be skipped by the reader, the system is tuned in §5, and the results of the numerical simulations are given in §6.

4. Dynamic model of the damping systems

4.1. Description and properties of the frames

In this paper, two frames are used: $\mathscr{R}_b \triangleq (CoG, \mathbf{x}_b, \mathbf{y}_b, \mathbf{z}_b)$ is the frame fixed to the barge, and $\mathscr{R}_n \triangleq (O, \mathbf{x}_n, \mathbf{y}_n, \mathbf{z}_n)$ is the Earth-fixed frame. Every vector $r \in \mathbb{R}^3$ is denoted by r^b when expressed in the b frame and r^n in $\mathscr{R}_n$. The frames are oriented such as $\mathbf{z}$ points downwards.

The orientation of $\mathscr{R}_b$ with respect to $\mathscr{R}_n$ is defined by the "roll-pitch-yaw" Euler triple denoted by $\Theta = [\varphi, \theta, \psi]^\top \in \mathbb{R}^3$ (See Fig. 4). The rotation matrix associated with Θ is

$$R(\Theta) \triangleq \begin{bmatrix} c_\psi c_\theta & -s_\psi c_\varphi + c_\psi s_\theta s_\varphi & s_\psi s_\varphi + c_\psi s_\theta c_\varphi \\ s_\psi c_\theta & c_\psi c_\varphi + s_\psi s_\theta s_\varphi & -c_\psi s_\varphi + s_\psi s_\theta c_\varphi \\ -s_\theta & c_\theta s_\varphi & c_\theta c_\varphi \end{bmatrix}$$

with $c_x = \cos(x)$ and $s_x = \sin(x)$.

Therefore, $\dot{\mathbf{x}}^n = R\mathbf{v}^b$, where $\mathbf{x}^n$ is the position of CoG in $\mathscr{R}_n$ expressed in the n frame, and $\mathbf{v}^b$ the velocity of $\mathscr{R}_b$ relatively to $\mathscr{R}_n$ and expressed in $\mathscr{R}_b$. For all $\mathbf{u} = [u_1, u_2, u_3]^\top \in \mathbb{R}^3$, we define the cross-product matrix as

$$S(\mathbf{u}) \triangleq \begin{bmatrix} 0 & -u_3 & u_2 \\ u_3 & 0 & -u_1 \\ -u_2 & u_1 & 0 \end{bmatrix} = -S(\mathbf{u})^\top$$

such that $\forall x, y \in \mathbb{R}^3$, $S(x)y = x \times y$. We denote by ω^b the rotation speed of the b frame relative to the n frame, expressed in $\mathscr{R}_b$. The time derivative of R can then be given by (Landau and Lifshitz, 1976)

$$\dot{R} = R\, S(\omega^b)$$

We define

$$G(\Theta) \triangleq \left[\mathbf{x}, R([\varphi, 0, 0]^\top)^\top \mathbf{y}, R(\Theta)^\top \mathbf{z}\right] = \begin{bmatrix} 1 & 0 & -s_\theta \\ 0 & c_\varphi & s_\varphi c_\theta \\ 0 & -s_\varphi & c_\varphi c_\theta \end{bmatrix} \tag{3}$$

such that $\omega^b = G\dot{\Theta}$, with $\mathbf{x}$, $\mathbf{y}$, $\mathbf{z}$ as the unit vector along each axis.

We define $q \triangleq \begin{bmatrix} \mathbf{x}^n \\ \Theta \\ w \end{bmatrix}$ and $v \triangleq \begin{bmatrix} \mathbf{v}^b \\ \boldsymbol{\omega}^b \\ \dot{w} \end{bmatrix}$, with $w \in \mathbb{R}^{nc}$ and nc the number of variables describing the speed of the liquid inside the TLCD (nc will be detailed in §4 for each variant). These variables are linked via $v = \mathscr{P}\dot{q}$ with

$$\mathscr{P}(\Theta) = \begin{bmatrix} R(\Theta)^\top & 0_{3\times 3} & 0_{3\times nc} \\ 0_{3\times 3} & G(\Theta) & 0_{3\times nc} \\ 0_{nc\times 3} & 0_{nc\times 3} & \mathbb{I}_{nc} \end{bmatrix}$$

We have described the geometry and kinematics of the system, and now establish the dynamics of our systems using the Lagrangian approach. The dynamics of the systems are classically given as

$$\frac{\mathrm{d}}{\mathrm{d}t}\frac{\partial(T-V)}{\partial \dot{q}} - \frac{\partial(T-V)}{\partial q} = Q$$

with T the kinetic energy, V the potential energy and Q the generalized forces.

4.2. Generalized forces

To obtain Q (the generalized forces), we express the power generated by external forces on our system as $\dot{q}^\top Q$. We write $Q \triangleq Q_{hydro} + Q_{res}$, with Q_{hydro} the generalized force due to the interactions between the waves and the barge, and Q_{res} the generalized force due to the restrictions in the TLMCD. For our simulations, the interactions between the platform and the water were modelled using a diffraction-radiation software. Following classical writing of the force generated by the fluid flow through the restriction, we write the forces $F_h \in \mathbb{R}^N$ in a damping system as

$$F_h = -\frac{1}{2}\rho A_h \eta \circ \mathscr{V}_h(\dot{w}) \circ \left|\mathscr{V}_h(\dot{w})\right|$$

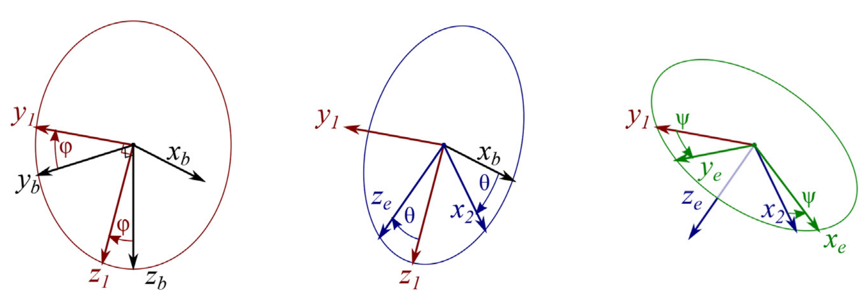

Fig. 4. Orientation of $\mathscr{R}_b$ with respect to $\mathscr{R}_e$.

with $\eta \in \mathbb{R}^N$ the vector of head-loss coefficients, ρ the fluid density, and ∘ the Hadamard product (entrywise product). To establish the expression for Q_{res}, we express the power dissipated by the restrictions as $P_{res} = \mathscr{V}_h^\top F_h$, with $\mathscr{V}_h^\top = \dot{w}^\top P_h^\top$ according to (2). Therefore, Q_{res} is given by

$$Q_{res}(t, \dot{w}) = \begin{bmatrix} 0_{6\times 1} \\ P_h^\top F_h(\dot{w}) \end{bmatrix} \tag{4}$$

4.3. System with N TLCDs (NU)

We consider N TLCDs regularly rotated around $(CoG, \mathbf{z}_b)$, and denote this system *NU*. As an example, the 2U system is illustrated in Fig. 5. We set $x_t^b = 0$ for our system to be axisymmetric. The orientation angle of each element writes $\alpha_i = \pi\frac{i-1}{N}$. To describe the position of the liquid, we need N variables, i.e. $nc = N$. For the *NU* system, each element is a TLCD, therefore, the curvilinear abscissa of each element, σ_i, ranges from $-\varsigma_{si}$ to ς_{pi} defined as

$$\varsigma_{pi} = \frac{L_h}{2} + L_v + w_i$$

$$\varsigma_{si} = \frac{L_h}{2} + L_v - w_i$$

4.3.1. Mechanical energy of the system

The potential energy of the *NU* system is written as

$$\begin{aligned} V_{NU} &= \mathbf{z}^\top . \left(g\rho \sum_{i=1}^{N} \int_{-\varsigma_{si}}^{\varsigma_{pi}} A_t(\sigma)\big(R(\Theta)R_z(\alpha_i)\mathbf{r}^b(\sigma) + \mathbf{x}^n\big)\mathrm{d}\sigma \right) \\ &= -gm_t z - g\rho\mathbf{z}^\top R(\Theta)\left[\rho \sum_{i=1}^{N} \int_{-\varsigma_{si}}^{\varsigma_{pi}} A_t(\sigma)R_z(\alpha_i)\mathbf{r}^b(\sigma)\mathrm{d}\sigma\right] \end{aligned} \tag{5}$$

where g is the acceleration due to gravity, m_t is the total mass of the liquid in the damping system.

The kinetic energy of the system is written as

$$T_{NU} = \frac{1}{2}\,\dot{q}^\top \mathscr{M}_{NU}(q)\,\dot{q} \tag{6}$$

with

$$\mathscr{M}_{NU}(q) \triangleq \mathscr{P}(\Theta)^\top M_{NU}(w)\,\mathscr{P}(\Theta) = \mathscr{M}_{NU}^\top \in \mathbb{R}^{6+nc\times 6+nc} \tag{7}$$

with $M_{NU}(w)$ as defined in (A.2). The calculation of the kinetic energy is detailed in Appendix A.1.

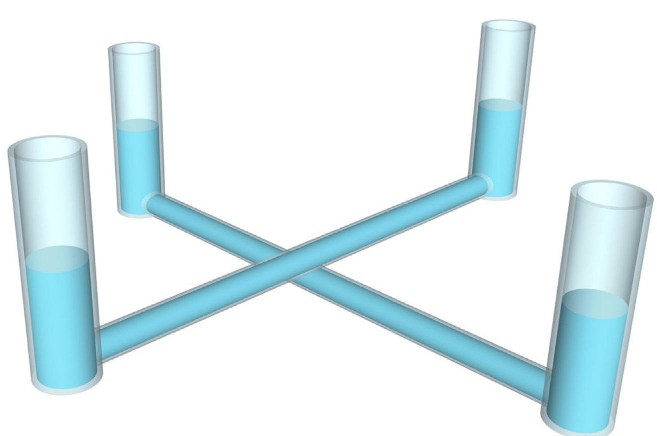

Fig. 5. Geometry of the 2U damping system (the tubes do not intersect).

4.3.2. System dynamics

We write the dynamics of the system as

$$\mathscr{M}_{NU}(q)\ddot{q} + C_{NU}(q,\dot{q})\dot{q} + k_{NU}(q) = Q_{hydro} + Q_{res_{NU}}(\dot{w}) \tag{8}$$

with $\mathscr{M}_{NU}(q)$ as defined in (7), and C_{NU}, k_{NU} and $Q_{res_{NU}}$ as defined in Appendix B.3.

4.4. Model of a star-shaped TLMCD with N elements (NS)

This damping system is composed of N halves of the TLCD interconnected at the coordinate $\mathbf{r}^b(\sigma = 0)$ and regularly rotated around $(CoG, \mathbf{z}_b)$. We denote this system *NS*. For illustration purpose, the 3S system is shown in Fig. 6.

For this system, each element is a half-TLCD, therefore the curvilinear abscissa of each element, σ_i, ranges from 0 to ς_i. We still consider $x_t^b = 0$. The orientation angle writes, $\alpha_i = \frac{2\pi(i-1)}{N}$.

We note $\sigma = \varsigma_i$, the coordinate of the free surface of the i^{th} element. The total mass of the liquid is constant, and can be given by

$$m_t \triangleq \rho \sum_{i=1}^{N} \int_0^{\varsigma_i} A_t(\sigma_i)\mathrm{d}\sigma_i$$

If we know ς_i for $i = 1,\ldots,N-1$, we can easily deduce ς_N; therefore, $nc = N-1$. We define, for $i = 1..nc$,

$$\varsigma_i = \frac{L_h}{2} + L_v + w_i, \tag{9}$$

and

$$\varsigma_N = \frac{L_h}{2} + L_v - \sum_{i=1}^{N-1} w_i. \tag{10}$$

As shown in Appendix B.4, we write the dynamics of the system as

$$\mathscr{M}_{NS}(q)\ddot{q} + C_{NS}(q,\dot{q})\dot{q} + k_{NS}(q) = Q_{hydro} + Q_{res_{NS}}(\dot{w}) \tag{11}$$

where $\mathscr{M}_{NS}$, C_{NS}, k_{NS} and $Q_{res_{NS}}$ are defined in Appendix B.4.

4.5. Model of polygonal TLMCD with N elements (NP)

This damping system is composed of N horizontal columns laid out to form a convex regular N-gon with N vertical columns positioned at each intersection. We denote his system *NP*. The 3P case is shown in Fig. 7.

The elements of this system are composed of one horizontal tube and one vertical column, therefore, the curvilinear abscissa of each element, σ_i, ranges from $-\frac{L_h}{2}$ to ς_i, as defined in (9). The geometry of our system implies $x_t^b = -\frac{L_h}{2\tan\frac{\pi}{N}}$. The orientation angle α_i writes $\alpha_i = \frac{2\pi(i-1)}{N}$, as in the *NS* problem.

There are $2N$ values of the speed of the liquid (one for each horizontal

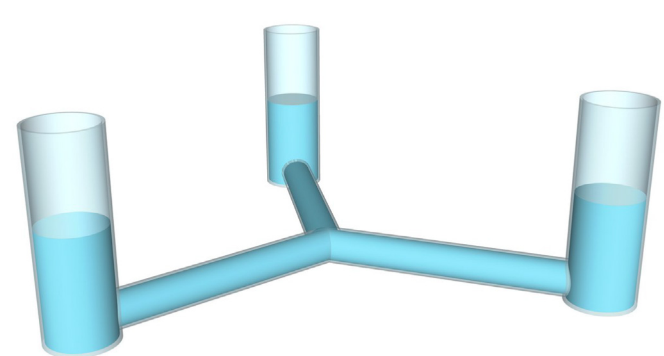

Fig. 6. The 3S TLMCD.

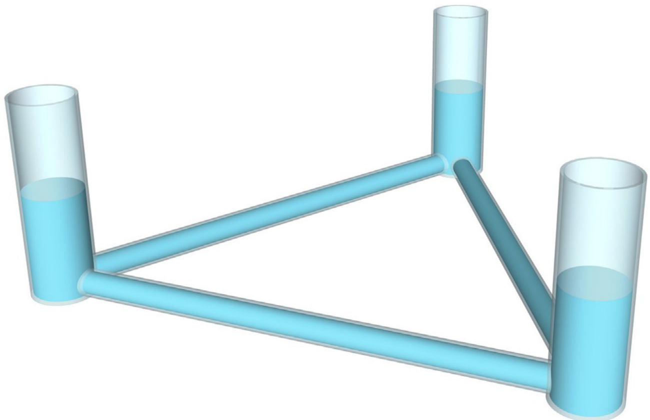

Fig. 7. The 3P TLMCD.

tube and each vertical column). We can write N local relations of flow conservation (at the base of each vertical column). We need $nc = 2N - N = N$ independent variables to know the speed of the liquid in each column. As the total mass of the liquid is constant, there are $N-1$ independent positions of free surfaces; therefore, we need to introduce an additional variable to completely describe the system. We arbitrarily choose w_{nc} to be the "position" of the liquid in the N^{th} horizontal column.

The system's equations of motion are written as

$$\mathcal{M}_{NP}(q)\,\ddot{q} + C_{NP}(q,\dot{q})\dot{q} + k_{NP}(q) = Q_{hydro} + Q_{res_{NP}}(\dot{w}) \tag{12}$$

where $\mathcal{M}_{NP}$, C_{NP}, k_{NP} and $Q_{res_{NP}}$ are defined in Appendix B.5.

4.6. Results frame

As we change the incidence of the waves, we need to change the results variables: we introduce φ_r the inline angular response and θ_r the transverse angular response to describe the oscillations of the FWT along the direction of the waves and perpendicular to the waves, respectively. We need to express φ_r and θ_r in terms of φ, θ and ψ. For this purpose, we introduced $\mathscr{R}_{er}$ and $\mathscr{R}_{br}$ as the "results frames". They are related via $R(\Theta_r)$ such that $\forall \mathbf{r} \in \mathbb{R}^3$,

$$\mathbf{r}^{er} = R(\Theta_r)\mathbf{r}^{br} \tag{13}$$

where $\Theta_r \triangleq [\varphi_r, \theta_r, \psi_r]^\top$. These frames are linked to $\mathscr{R}_e$ and $\mathscr{R}_b$ by a rotation around $\mathbf{z}$ at angle β, such that $\forall \mathbf{r} \in \mathbb{R}^3$,

$$\mathbf{r}^e = R_z(\beta)\mathbf{r}^{er}$$

and

$$\mathbf{r}^b = R_z(\beta)\mathbf{r}^{br}.$$

In §4.1 we defined $R(\Theta)$ so that

$$\mathbf{r}^e = R(\Theta)\mathbf{r}^b$$

thus, we write

$$\mathbf{r}^{er} = R_z^\top(\beta)\mathbf{r}^e = R_z^\top(\beta)R(\Theta)\mathbf{r}^b = R_z^\top(\beta)R(\Theta)R_z(\beta)\mathbf{r}^{br},$$

and by identification with (13), we get

$$R(\Theta_r) = R_z^\top(\beta)R(\Theta)R_z(\beta). \tag{14}$$

Solving this equation yields Θ_r in terms of Θ and β.

Table 4
Optimal TLMCD parameters for a wave height $H = 3$ m.

	ν	η	L_h	A_v	μ	$P.I.$
2U	4.06	5.90	32.31 m	5.68 m^2	4%	3.50
3S	4.12	3.43	31.88 m	7.67 m^2	4%	3.57
3P	7.11	10.72	27.61 m	7.65 m^2	4%	3.54

5. Tuning the proposed configurations

Prior to assessing the robustness of each solution against wave incidence, we need to determine their design parameters. First, we must determine the mass of the liquid in the damper. We arbitrarily assume that each TLCD of the 2U variant weighs 2% of the total mass of the float, and that each TLMCD weighs 4% of the total mass, i.e. 2U, 3S and 3P have the same mass. According to (Yalla, 2001), the price of the system depends on three factors: the loss of space (occupied by the TLCD), additional construction costs, and the amount of steel needed for the tank. Since the space inside the barge has no commercial value, the cost of the loss of space is zero (if the system to damp was a building, the cost due to loss of space would have been the price of the floors occupied by the device). In our case, if the vertical columns were outside the float, additional construction costs would have incurred to ensure the structural integrity of the TLCD. To reduce this cost to zero, we designed the dampers to fit inside the barge. To determine the best design of each damper, we use the MATLAB fminsearch optimisation function, with the following performance index to be minimized:

$$P.I. = \max_{T\in[3;30]}(|\varphi|)$$

where $|\varphi|$ is the steady state roll magnitude obtained via a simulation for each period of monochromatic wave (excitation). It is a *min-max* problem where the decision variables are L_h, L_v, ν and η. This problem is solved under constraints $L_h \le L_{h_{maxi}}$ and $L_v \le L_{v_{maxi}}$ to fit the damper inside the barge so that the construction cost remains zero. To avoid a violation of assumption 6, we set $L_v = L_{v_{maxi}}$.

In a previous paper (Coudurier et al., 2015), we considered damping with a single TLCD using the same float subject to waves in the vertical plan $x_t = 0$. The results showed that the optimal value of L_h was $L_{h_{maxi}}$. Therefore, we chose to set $L_h = L_{h_{maxi}}$ to reduce the number of variables in the optimization problem. As we have $L_h = L_{h_{maxi}}$ and $L_v = L_{v_{maxi}}$, the position of the TLMCD inside the barge is imposed.

We define $\mu \triangleq \frac{m_t}{M_{S_{11}}}$ as the ratio of the mass of the liquid in the TLMCD to the total mass of the float. We summarize the design of each damper in Table 4 for a given wave height $H = 3$ m and an incidence of $\beta = 0°$.

As the natural period of the float is close to the predominant period of extreme sea states (15 s–20 s), we chose the performance index to damp this resonance. Note that for a given site, we could have used an adapted performance index to obtain the design best suited to the conditions of the local sea.

We also note that ν (the cross-section ratio) of the 3P system is much larger, which means that the 3P system has a lower resonant period for the same ν.

6. Simulation results

In the previous section we detailed the design of each damping system. In this section we perform numerical simulations to compare their robustness against wave incidence. As the dampers are tuned to the roll/pitch natural frequency, they have almost no effect on the other motions of the wind turbine. This is why in this section we only deal with the roll and pitch motions.

6.1. Preliminary considerations

Before we perform numerical simulations, let's consider the following points.

Evaluation criterion: The RAO We introduce the response amplitude operator (RAO). It is defined as the ratio of the system's motion to the wave amplitude causing it, and is represented over a range of (monochromatic) wave periods (International Organization for Standardization, 2009). It is employed as a quantitative evaluation tool for the rest of the study.

Results frames We remind the reader that we introduced the results frame in §4.6. As we use the linear model, the states of the results frame are linked to the original states via $\mathbf{x}^{nr} = R_z^\top(\beta)\mathbf{x}^n$ and $\Theta^r = R_z^\top(\beta)\Theta$.

6.2. Numerical simulations

We simulated the system's response to a 3 m wave excitation until a steady state was attained. We plotted the RAOs for monochromatic waves of periods ranging from 3 s to 30 s as well as for different incident angles. It has been verified that the vertical columns were never empty during

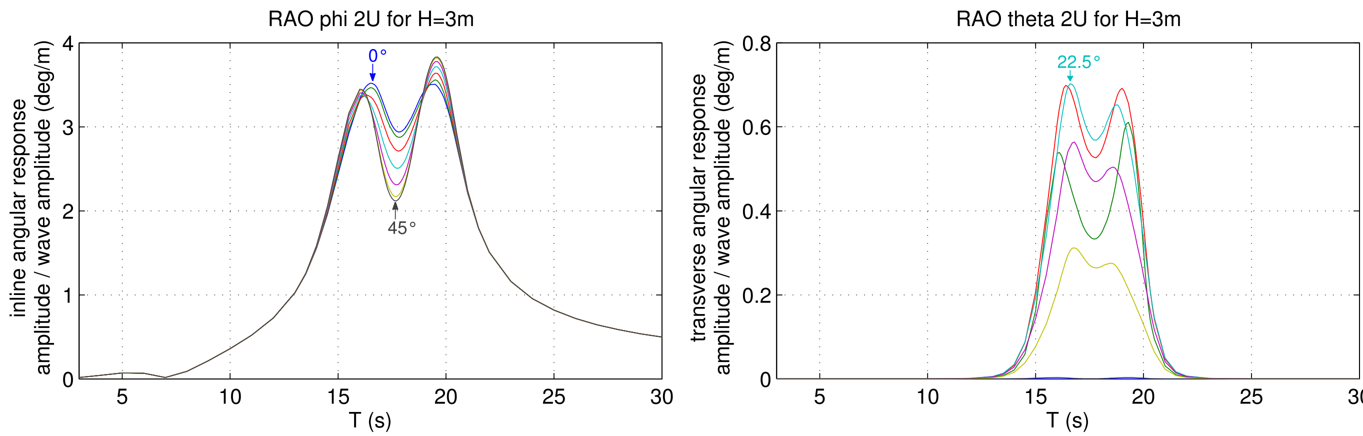

(a) RAO of the 2U system

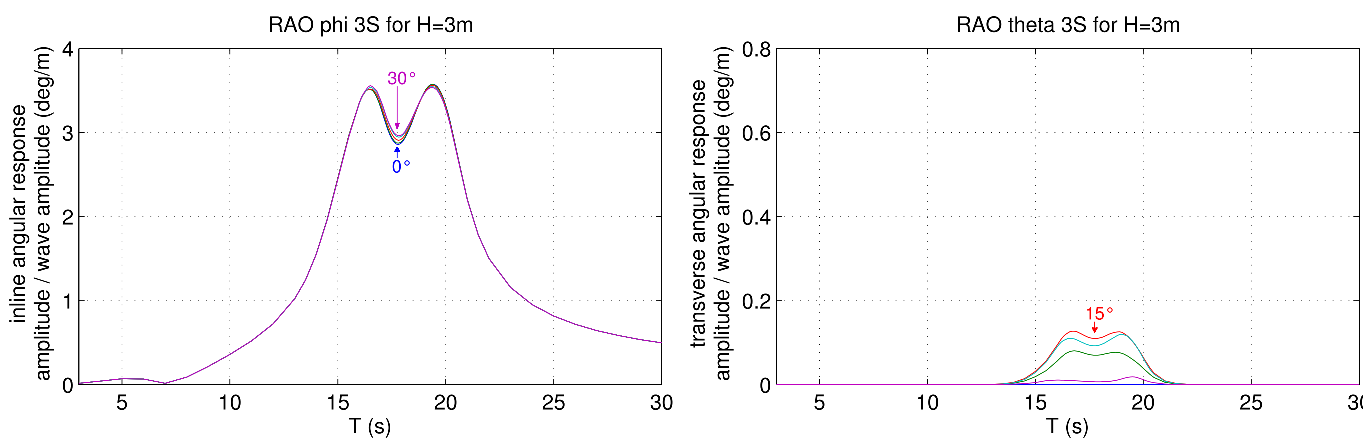

(b) RAO of the 3S system

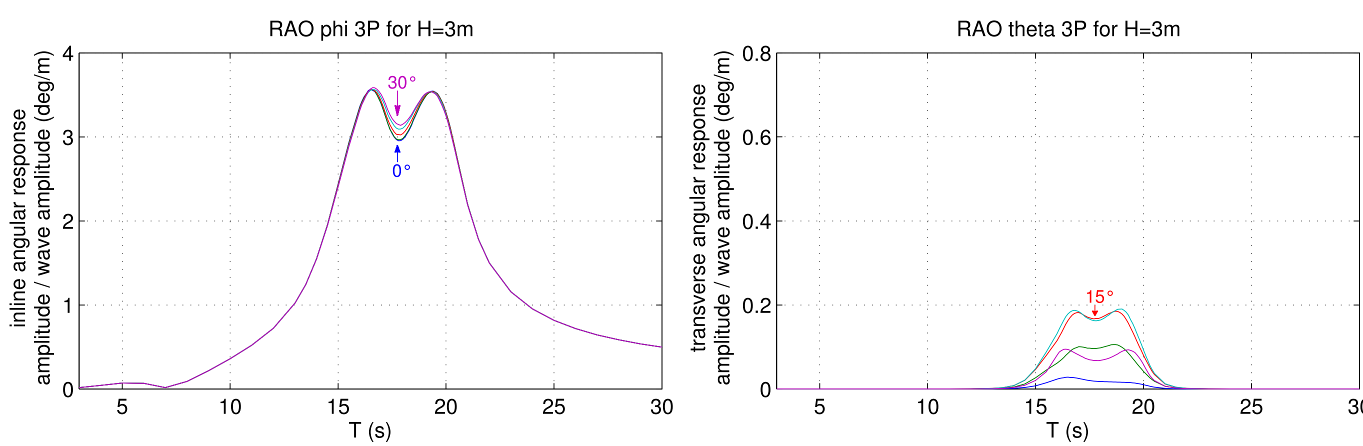

(c) RAO of the 3P system

Fig. 8. RAO of an arrangement of multiple TLCDs (a) and variants of TLMCDs ((b) and (c)) for different wave incidences of a 3 m monochromatic wave.

the simulations.

We plotted the results in Fig. 8. Due to the symmetries of the damping systems, we plotted curves between 0° and 45° for the 2U case, and between 0° and 30° for the 3S and 3P cases.

In Fig. 8, we can see that the 3S and 3P systems are more robust against wave incidence than the 2U damper. All dampers create a parasitic transverse angular response, but it is worth noting that the 2U system creates significantly greater parasitic transverse angular motion than the 3P and 3S dampers.

7. Conclusions

In this paper, we introduced the concept of a tuned liquid multi-column damper to damp systems with similar pitch and roll behaviours, e.g. an offshore platform. This damper was inspired by the tuned liquid column damper (TLCD). We developed dynamic models of an offshore platform coupled with different variants of TLMCDs and compared them against a reference system consisting of an arrangement of multiple TLCDs. The results of simulations showed that the two proposed systems (3S and 3P) are more robust against variations in wave incidence than a crosswise layout of two TLCDs.

In this study, all considered devices are passive. However further work will focus on the semi-active control of these devices, i.e. changing the head loss coefficients η continually to achieve better performance.

Appendix A. Kinetic and potential energy of the proposed dampers

Appendix A.1. Kinetic energy of the NU damper

Following the method used in [8, Appendix B], we compute the kinetic energy of the *NU* system.

For the *N*U system and for $i = 1, \ldots, N$

$$v_i(\sigma_i) = \frac{A_v}{A_t(\sigma_i)} \dot{w}_i,$$

we write $\mathbf{v}_i^b(\sigma_i)$ according to (1)

$$\mathbf{v}_i^b(\sigma_i) = \frac{A_v}{A_t(\sigma_i)} \dot{w}_i R_z(\alpha_i) \frac{\mathrm{d}\mathbf{r}^b}{\mathrm{d}\sigma}(\sigma_i).$$

Therefore, matrix $P_{h_{NU}}$ appearing in (2) can be given by

$$P_{h_{NU}} = \nu \mathbb{I}_{nc}$$

We write the kinetic energy of the system as

$$T_{NU} = T_s + T_{DNU},$$

where

$$T_s = \frac{1}{2} v^\top \begin{bmatrix} M_s & 0_{6\times nc} \\ 0_{nc\times 6} & 0_{nc\times nc} \end{bmatrix} v$$

with M_s the float mass matrix, and

$$\begin{aligned} T_{DNU} &= \frac{1}{2}\rho \sum_{i=1}^{N} \int_{-\varsigma_{si}}^{\varsigma_{pi}} A_t(\sigma_i) \left\| \mathbf{v}^b + \boldsymbol{\omega}^b \times R_z(\alpha_i)\mathbf{r}^b(\sigma_i) + \mathbf{v}_i^b(\sigma_i) \right\|^2 \mathrm{d}\sigma_i \\ &= \frac{1}{2}\sum_{i=1}^{N}\left(\rho \int_{-\varsigma_{si}}^{\varsigma_{pi}} A_t(\sigma_i)\mathrm{d}\sigma_i\right) \left|\left|\mathbf{v}^b\right|\right|^2 - \frac{1}{2}\boldsymbol{\omega}^{b\top}\left(\rho \sum_{i=1}^{N} \int_{-\varsigma_{si}}^{\varsigma_{pi}} A_t(\sigma_i) S^2\left(R_z(\alpha_i)\mathbf{r}^b(\sigma_i)\right)\mathrm{d}\sigma_i\right)\boldsymbol{\omega}^b \\ &+\boldsymbol{\omega}^{b\top}\left(\rho \sum_{i=1}^{N} \int_{-\varsigma_{si}}^{\varsigma_{pi}} A_t(\sigma_i) S\left(R_z(\alpha_i)\mathbf{r}^b(\sigma_i)\right)\mathrm{d}\sigma_i\right)\mathbf{v}^b + \mathbf{v}^{b\top}\left(\rho A_v \sum_{i=1}^{N} \int_{-\varsigma_{si}}^{\varsigma_{pi}} R_z(\alpha_i)\frac{\mathrm{d}\mathbf{r}^b}{\mathrm{d}\sigma}(\sigma_i)\dot{w}_i \mathrm{d}\sigma_i\right) \\ &+\boldsymbol{\omega}^{b\top}\left(\rho A_v \sum_{i=1}^{N} \int_{-\varsigma_{si}}^{\varsigma_{pi}} S\left(R_z(\alpha_i)\mathbf{r}^b(\sigma_i)\right)R_z(\alpha_i)\frac{\mathrm{d}\mathbf{r}^b}{\mathrm{d}\sigma}(\sigma_i)\dot{w}_i\mathrm{d}\sigma_i\right) \\ &+\frac{1}{2}\sum_{i=1}^{N}\left(\rho A_v^2 \int_{-\varsigma_{si}}^{\varsigma_{pi}} \frac{\dot{w}_i^2}{A_t(\sigma_i)}\mathrm{d}\sigma_i\right). \end{aligned}$$

Therefore, we can write

$$T_{NU} = \frac{1}{2} v^\top M_{NU}(w) v = \frac{1}{2}\dot{q}^\top \mathscr{M}_{NU}(q)\dot{q}, \tag{A.1}$$

with $\mathscr{M}_{NU} \triangleq \mathscr{P}^\top M_{NU}\mathscr{P}$ and

$$M_{NU}(w) \triangleq \begin{bmatrix} M_s & 0_{6\times nc} \\ 0_{nc\times 6} & 0_{nc\times nc} \end{bmatrix} + \begin{bmatrix} m_t \mathbb{I}_3 & M_{v\omega}(w) & M_{vq}(w) \\ M_{v\omega}^\top(w) & M_\omega(w) & M_{\omega q}(w) \\ M_{vq}^\top(w) & M_{\omega q}^\top(w) & M_q(w) \end{bmatrix}. \tag{A.2}$$

For $i = 1, \dots, nc$,

$$m_t \triangleq \rho \sum_{i=1}^{N} \int_{-\varsigma_{si}}^{\varsigma_{pi}} A_t(\sigma_i)\mathrm{d}\sigma_i \in \mathbb{R}$$

$$M_{v\omega} \triangleq -\rho \sum_{i=1}^{N} \int_{-\varsigma_{si}}^{\varsigma_{pi}} A_t(\sigma_i) S\big(R_z(\alpha_i)\mathbf{r}^b(\sigma_i)\big)\mathrm{d}\sigma_i = -M_{v\omega}^\top(w) \in \mathbb{R}^{3\times 3}$$

$$M_\omega \triangleq -\rho \sum_{i=1}^{N} \int_{-\varsigma_{si}}^{\varsigma_{pi}} A_t(\sigma_i) S^2\big(R_z(\alpha_i)\mathbf{r}^b(\sigma_i)\big)\mathrm{d}\sigma_i = M_\omega^\top(w) \in \mathbb{R}^{3\times 3}$$

$$M_{vq}[\,:, i] \triangleq \rho A_v \int_{-\varsigma_{si}}^{\varsigma_{pi}} R_z(\alpha_i)\frac{\mathrm{d}\mathbf{r}^b}{\mathrm{d}\sigma}(\sigma_i)\mathrm{d}\sigma_i \in \mathbb{R}^{3\times 1}$$

$$M_{\omega q}[\,:, i] \triangleq \rho A_v \int_{-\varsigma_{si}}^{\varsigma_{pi}} S\big(R_z(\alpha_i)\mathbf{r}^b(\sigma_i)\big)R_z(\alpha_i)\frac{\mathrm{d}\mathbf{r}^b}{\mathrm{d}\sigma}(\sigma_i)\mathrm{d}\sigma \in \mathbb{R}^{3\times 1}$$

$$M_q \triangleq \mathbb{I}_{nc}\rho A_v(L_h\nu + 2L_v) \in \mathbb{R}^{nc}$$

with $M_{vq} \in \mathbb{R}^{3\times nc}$, $M_{\omega q} \in \mathbb{R}^{3\times nc}$.

Appendix A.2. Kinetic and potential energy of the NS damper

Following the method used in Appendix A.1 for the *NS* variant, we write

$$M_{NS}(w) \triangleq \begin{bmatrix} M_s & 0_{6\times nc} \\ 0_{nc\times 6} & 0_{nc\times nc} \end{bmatrix} + \begin{bmatrix} m_t \mathbb{I}_3 & M_{v\omega}(w) & M_{vq}(w) \\ M_{v\omega}^\top(w) & M_\omega(w) & M_{\omega q}(w) \\ M_{vq}^\top(w) & M_{\omega q}^\top(w) & M_q(w) \end{bmatrix}$$

with, for $j = 1, \dots, nc$,

$$m_t \triangleq \rho \sum_{i=1}^{N} \int_{0}^{\varsigma_i} A_t(\sigma_i)\mathrm{d}\sigma_i \in \mathbb{R}$$

$$M_{v\omega} \triangleq -\rho \sum_{i=1}^{N} \int_{0}^{\varsigma_i} A_t(\sigma_i) S\big(R_z(\alpha_i)\mathbf{r}^b(\sigma_i)\big)\mathrm{d}\sigma_i = -M_{v\omega}^\top(w) \in \mathbb{R}^{3\times 3}$$

$$M_\omega \triangleq -\rho \sum_{i=1}^{N} \int_{0}^{\varsigma_i} A_t(\sigma_i) S^2\big(R_z(\alpha_i)\mathbf{r}^b(\sigma_i)\big)\mathrm{d}\sigma_i = M_\omega^\top(w) \in \mathbb{R}^{3\times 3}$$

$$M_{vq}[\,:, j] \triangleq \rho A_v P_{h_{NS}}[\,:, j] \sum_{i=1}^{N} \int_{0}^{\varsigma_i} R_z(\alpha_i)\frac{\mathrm{d}\mathbf{r}^b}{\mathrm{d}\sigma}(\sigma_i)\mathrm{d}\sigma_i \in \mathbb{R}^{3\times 1}$$

$$M_{\omega q}[\,:, j] \triangleq \rho A_v P_{h_{NS}}[\,:, j] \sum_{i=1}^{N} \int_{0}^{\varsigma_i} S\big(R_z(\alpha_i)\mathbf{r}^b(\sigma_i)\big)R_z(\alpha_i)\frac{\mathrm{d}\mathbf{r}^b}{\mathrm{d}\sigma}(\sigma_i)\mathrm{d}\sigma \in \mathbb{R}^{3\times 1}$$

$$M_q \triangleq \rho A_v \left(P_{h_{NS}}^\top \frac{L_h}{2\nu}(\nu - 1) + \nu^{-2} P_{h_{NS}}^\top \begin{bmatrix} \varsigma_1 & 0 & \cdots & \cdots & 0 \\ 0 & \ddots & \ddots & & \vdots \\ \vdots & \ddots & \ddots & \ddots & \vdots \\ \vdots & & \ddots & \ddots & 0 \\ 0 & \cdots & \cdots & 0 & \varsigma_N \end{bmatrix} P_{h_{NS}} \right) \in \mathbb{R}^{nc}$$

with $M_{vq} \in \mathbb{R}^{3\times nc}$, $M_{\omega q} \in \mathbb{R}^{3\times nc}$, and

$$P_{h_{NS}} \triangleq \nu \begin{bmatrix} \mathbb{I}_{nc} \\ -1_{1\times nc} \end{bmatrix}.$$

The potential energy of the NS system is written as

$$V_{NS} = \mathbf{z}^{\top}.\left(g\rho\sum_{i=1}^{N}\int_{0}^{\varsigma_i} A_t(\sigma)\big(R(\Theta)\,R_z(\alpha_i)\mathbf{r}^b(\sigma)+\mathbf{x}^n\big)\mathrm{d}\sigma\right) = -gm_t z - g\rho\mathbf{z}^{\top}R(\Theta)\left[\rho\sum_{i=1}^{N}\int_{0}^{\varsigma_i} A_t(\sigma)R_z(\alpha_i)\mathbf{r}^b(\sigma)\mathrm{d}\sigma\right] \tag{A.3}$$

Appendix A.3. Kinetic and potential energy of the NP damper

Following the method used in Appendix A.1 for the NP variant, we write

$$M_{NP}(w) \triangleq \begin{bmatrix} M_s & 0_{6\times nc} \\ 0_{nc\times 6} & 0_{nc\times nc}\end{bmatrix} + \begin{bmatrix} m_t\mathbb{I}_3 & M_{v\omega}(w) & M_{vq}(w) \\ M_{v\omega}^{\top}(w) & M_{\omega}(w) & M_{\omega q}(w) \\ M_{vq}^{\top}(w) & M_{\omega q}^{\top}(w) & M_q(w)\end{bmatrix}$$

with, for $j = 1,\ldots,nc$,

$$m_t \triangleq \rho\sum_{i=1}^{N}\int_{-\frac{L_h}{2}}^{\varsigma_i} A_t(\sigma_i)\mathrm{d}\sigma_i \in \mathbb{R}$$

$$M_{v\omega} \triangleq -\rho\sum_{i=1}^{N}\int_{-\frac{L_h}{2}}^{\varsigma_i} A_t(\sigma_i)S\big(R_z(\alpha_i)\mathbf{r}^b(\sigma_i)\big)\mathrm{d}\sigma_i = -M_{v\omega}^{\top}(w) \in \mathbb{R}^{3\times 3}$$

$$M_{\omega} \triangleq -\rho\sum_{i=1}^{N}\int_{-\frac{L_h}{2}}^{\varsigma_i} A_t(\sigma_i)S^2\big(R_z(\alpha_i)\mathbf{r}^b(\sigma_i)\big)\mathrm{d}\sigma_i = M_{\omega}^{\top}(w) \in \mathbb{R}^{3\times 3}$$

$$M_{vq}[\,:,j] \triangleq \rho A_v P_{h_{NP}}[\,:,j]\sum_{i=1}^{N}\int_{-\frac{L_h}{2}}^{\frac{L_h}{2}} R_z(\alpha_i)\frac{\mathrm{d}\mathbf{r}^b}{\mathrm{d}\sigma}(\sigma_i)\mathrm{d}\sigma_i + \rho A_v P_{h2_{NP}}[\,:,j]\sum_{i=1}^{N}\int_{\frac{L_h}{2}}^{\varsigma_i} R_z(\alpha_i)\frac{\mathrm{d}\mathbf{r}^b}{\mathrm{d}\sigma}(\sigma_i)\mathrm{d}\sigma_i \in \mathbb{R}^{3\times 1}$$

$$M_{\omega q}[\,:,j] \triangleq \rho A_v P_{h_{NP}}[\,:,j]\sum_{i=1}^{N}\int_{-\frac{L_h}{2}}^{\frac{L_h}{2}} S\big(R_z(\alpha_i)\mathbf{r}^b(\sigma_i)\big)R_z(\alpha_i)\frac{\mathrm{d}\mathbf{r}^b}{\mathrm{d}\sigma}(\sigma_i)\mathrm{d}\sigma + \rho A_v P_{h2_{NP}}[\,:,j]\sum_{i=1}^{N}\int_{\frac{L_h}{2}}^{\varsigma_i} S\big(R_z(\alpha_i)\mathbf{r}^b(\sigma_i)\big)R_z(\alpha_i)\frac{\mathrm{d}\mathbf{r}^b}{\mathrm{d}\sigma}(\sigma_i)\mathrm{d}\sigma \in \mathbb{R}^{3\times 1}$$

$$M_q \triangleq \rho A_v\left(\frac{L_h}{\nu}P_{h_{NP}}^{\top}P_{h_{NP}} + \nu^{-2}P_{h2_{NP}}^{\top}\begin{bmatrix} \varsigma_1-\frac{L_h}{2} & 0 & \cdots & \cdots & 0 \\ 0 & \ddots & \ddots & & \vdots \\ \vdots & \ddots & \ddots & \ddots & \vdots \\ \vdots & & \ddots & \ddots & 0 \\ 0 & \cdots & \cdots & 0 & \varsigma_N-\frac{L_h}{2}\end{bmatrix}P_{h2_{NP}}\right) \in \mathbb{R}^{nc}$$

with $M_{vq} \in \mathbb{R}^{3\times nc}$, $M_{\omega q} \in \mathbb{R}^{3\times nc}$, and

$$P_{h2_{NP}} \triangleq \begin{bmatrix} \mathbb{I}_{N-1} & 0_{N-1\times 1} \\ -1_{1\times N-1} & 0\end{bmatrix}$$

$$P_{h_{NP}} \triangleq \begin{bmatrix} \nu & 0 & \cdots & 0 & 1 \\ \nu & \ddots & \ddots & \vdots & \vdots \\ \vdots & \ddots & \ddots & 0 & 1 \\ \nu & \cdots & \nu & \nu & 1 \\ 0 & \cdots & 0 & 0 & 1\end{bmatrix}.$$

The potential energy of the NP system is written as

$$V_{NP} = \mathbf{z}^{\top}.\left(g\rho\sum_{i=1}^{N}\int_{-\frac{L_h}{2}}^{\varsigma_i} A_t(\sigma)\big(R(\Theta)\,R_z(\alpha_i)\mathbf{r}^b(\sigma)+\mathbf{x}^n\big)\mathrm{d}\sigma\right) = -gm_t z - g\rho\mathbf{z}^{\top}R(\Theta)\left[\rho\sum_{i=1}^{N}\int_{-\frac{L_h}{2}}^{\varsigma_i} A_t(\sigma)R_z(\alpha_i)\mathbf{r}^b(\sigma)\mathrm{d}\sigma\right] \tag{A.4}$$

Appendix B. Derivation of system dynamics

Appendix B.1. Preliminary results

For our calculation, we need the following results:

We define the derivative of row vector $x^\top \triangleq [x_1 \quad \dots \quad x_n]$ by column vector $y \triangleq \begin{bmatrix} y_1 \\ \vdots \\ y_m \end{bmatrix}$ as

$$\frac{\partial x^\top}{\partial y} \triangleq \begin{bmatrix} \frac{\partial x_1}{\partial y_1} & \cdots & \frac{\partial x_n}{\partial y_1} \\ \vdots & \ddots & \vdots \\ \frac{\partial x_1}{\partial y_m} & \cdots & \frac{\partial x_n}{\partial y_m} \end{bmatrix}. \tag{B.1}$$

Proposition 1. *$\forall \mathbf{r} \in \mathbb{R}^3$, the derivative of $\mathbf{r}^\top R$ by Θ is given as*

$$\frac{\partial \mathbf{r}^\top R}{\partial \Theta} = -G^\top S(R^\top \mathbf{r}) \tag{B.2}$$

with G as defined in (??), and $S(\cdot)$ is the matrix associated with the cross-product. We detail the calculus for each of the tree base vectors $(\mathbf{x}, \mathbf{y}, \mathbf{z})$. We have

$$R^\top \mathbf{z} = \begin{bmatrix} -s_\theta \\ s_\varphi c_\theta \\ c_\varphi c_\theta \end{bmatrix}$$

so

$$-G^\top S(R^\top \mathbf{z}) = \begin{bmatrix} 0 & c_\theta c_\varphi & -c_\theta s_\varphi \\ -c_\theta & -s_\theta s_\varphi & -s_\theta c_\varphi \\ 0 & 0 & 0 \end{bmatrix}$$

and

$$\frac{\partial \mathbf{z}^\top R}{\partial \Theta} = \begin{bmatrix} 0 & c_\theta c_\varphi & -c_\theta s_\varphi \\ -c_\theta & -s_\theta s_\varphi & -s_\theta c_\varphi \\ 0 & 0 & 0 \end{bmatrix}.$$

Therefore,

$$\frac{\partial \mathbf{z}^\top R}{\partial \Theta} = -G^\top S(R^\top \mathbf{z}).$$

We also have

$$R^\top \mathbf{y} = \begin{bmatrix} c_\theta s_\psi \\ c_\varphi c_\psi + s_\varphi s_\theta s_\psi \\ -s_\varphi c_\psi + c_\varphi s_\theta s_\psi \end{bmatrix}$$

so,

$$-G^\top S(R^\top \mathbf{y}) = \begin{bmatrix} 0 & -s_\varphi c_\psi + c_\varphi s_\theta s_\psi & -c_\varphi c_\psi - s_\varphi s_\theta s_\psi \\ -s_\theta s_\psi & s_\varphi c_\theta s_\psi & c_\varphi c_\theta s_\psi \\ c_\theta c_\psi & -c_\varphi s_\psi + s_\varphi s_\theta c_\psi & s_\varphi s_\psi + c_\varphi s_\theta c_\psi \end{bmatrix}$$

and

$$\frac{\partial \mathbf{y}^\top R}{\partial \Theta} = \begin{bmatrix} 0 & -s_\varphi c_\psi + c_\varphi s_\theta s_\psi & -c_\varphi c_\psi - s_\varphi s_\theta s_\psi \\ -s_\theta s_\psi & s_\varphi c_\theta s_\psi & c_\varphi c_\theta s_\psi \\ c_\theta c_\psi & -c_\varphi s_\psi + s_\varphi s_\theta c_\psi & s_\varphi s_\psi + c_\varphi s_\theta c_\psi \end{bmatrix}.$$

Therefore,

$$\frac{\partial \mathbf{y}^\top R}{\partial \Theta} = -G^\top S(R^\top \mathbf{y}).$$

Finally,

$$R^\top \mathbf{x} = \begin{bmatrix} c_\theta c_\psi \\ -c_\varphi s_\psi + s_\varphi s_\theta c_\psi \\ s_\varphi s_\psi + c_\varphi s_\theta c_\psi \end{bmatrix}$$

so,

$$-G^\top S(R^\top \mathbf{x}) = \begin{bmatrix} 0 & s_\varphi s_\psi + c_\varphi s_\theta c_\psi & c_\varphi s_\psi - s_\varphi s_\theta c_\psi \\ -s_\theta c_\psi & s_\varphi c_\theta c_\psi & c_\varphi c_\theta c_\psi \\ -c_\theta s_\psi & -c_\varphi c_\psi - s_\varphi s_\theta s_\psi & s_\varphi c_\psi - c_\varphi s_\theta s_\psi \end{bmatrix}$$

and

$$\frac{\partial \mathbf{x}^\top R}{\partial \Theta} = \begin{bmatrix} 0 & s_\varphi s_\psi + c_\varphi s_\theta c_\psi & c_\varphi s_\psi - s_\varphi s_\theta c_\psi \\ -s_\theta c_\psi & s_\varphi c_\theta c_\psi & c_\varphi c_\theta c_\psi \\ -c_\theta s_\psi & -c_\varphi c_\psi - s_\varphi s_\theta s_\psi & s_\varphi c_\psi - c_\varphi s_\theta s_\psi \end{bmatrix}.$$

Therefore,

$$\frac{\partial \mathbf{x}^\top R}{\partial \Theta} = -G^\top S(R^\top \mathbf{x}).$$

With $\mathbf{r} = r_1 \mathbf{x} + r_2 \mathbf{y} + r_3 \mathbf{z}$, by linearity,

$$\frac{\partial \mathbf{r}^\top R}{\partial \Theta} = -G^\top S(R^\top \mathbf{r}).$$

Proposition 2. *The derivatives of* $\mathbf{v}^{b\top}$ *and* $\boldsymbol{\omega}^{b\top}$ *by* Θ *are*

$$\frac{\partial \mathbf{v}^{b\top}}{\partial \Theta} = -G^\top S(\mathbf{v}^b) \tag{B.3}$$

$$\frac{\partial \boldsymbol{\omega}^{b\top}}{\partial \Theta} = \dot{G}^\top - G^\top S(\boldsymbol{\omega}^b). \tag{B.4}$$

Hence,

$$\boldsymbol{\omega}^b = G(\Theta)\dot{\Theta} = \begin{bmatrix} \dot{\varphi} + s_\theta \dot{\psi} \\ c_\theta s_\varphi \dot{\psi} + c_\varphi \dot{\theta} \\ c_\theta c_\varphi \dot{\psi} - s_\varphi \dot{\theta} \end{bmatrix}$$

so,

$$\frac{\partial \boldsymbol{\omega}^{b\top}}{\partial \Theta} = \begin{bmatrix} 0 & c_\theta c_\varphi \dot{\psi} - s_\varphi \dot{\theta} & -c_\theta s_\varphi \dot{\psi} - c_\varphi \dot{\theta} \\ -c_\theta \dot{\psi} & -s_\theta s_\varphi \dot{\psi} & -s_\theta c_\varphi \dot{\psi} \\ 0 & 0 & 0 \end{bmatrix}$$

With G as defined in (??),

$$\dot{G}^\top = \begin{bmatrix} 0 & 0 & 0 \\ 0 & -s_\varphi \dot{\varphi} & -c_\varphi \dot{\varphi} \\ -c_\theta \dot{\theta} & c_\theta c_\varphi \dot{\varphi} - s_\theta s_\varphi \dot{\theta} & -c_\theta s_\varphi \dot{\varphi} - s_\theta c_\varphi \dot{\theta} \end{bmatrix}.$$

We also write

$$G^\top S(G(\Theta)\dot{\Theta}) = \begin{bmatrix} 0 & -c_\theta c_\varphi \dot{\psi} + s_\varphi \dot{\theta} & c_\theta s_\varphi \dot{\psi} + c_\varphi \dot{\theta} \\ c_\theta \dot{\psi} & s_\varphi(-\dot{\varphi} + s_\theta \dot{\psi}) & c_\varphi(-\dot{\varphi} + s_\theta \dot{\psi}) \\ -c_\theta \dot{\theta} & c_\theta c_\varphi \dot{\varphi} - s_\theta s_\varphi \dot{\theta} & -c_\theta s_\varphi \dot{\varphi} - s_\theta c_\varphi \dot{\theta} \end{bmatrix}.$$

Therefore,

$$\frac{\partial \boldsymbol{\omega}^{b\top}}{\partial \Theta} = \dot{G}^\top - G^\top S(\boldsymbol{\omega}^b).$$

As $\mathbf{v}^b$ is $R^\top \dot{\mathbf{x}}^e$, according to Proposition 1,

$$\frac{\partial \mathbf{v}^{b\top}}{\partial \Theta} = -G^\top S(\mathbf{v}^b).$$

Appendix B.2. Derivation of the dynamics for the NU system

Using a Lagrangian approach, the dynamics of the system are given by

$$\frac{\mathrm{d}}{\mathrm{d}t}\frac{\partial (T_{NU} - V_{NU})}{\partial \dot{q}} - \frac{\partial (T_{NU} - V_{NU})}{\partial q} = Q$$

We first derive $\frac{\partial T_{NU}}{\partial q}$. According to (A.1), T is independent of x^n; therefore,

$$\frac{\partial T_{NU}}{\partial x^n} = 0_{3\times 1}.$$

As M is symmetrical and is not a function of Θ,

$$\frac{\partial T_{NU}}{\partial \Theta} = \frac{1}{2}\frac{\partial (\dot{q}^\top \mathscr{P}^\top M_{NU} \mathscr{P}\dot{q})}{\partial \Theta} = \frac{\partial (\mathscr{P}\dot{q})^\top}{\partial \Theta} M_{NU}(\mathscr{P}\dot{q}).$$

Using (B.3) and (B.4),

$$\frac{\partial (\mathscr{P}\dot{q})^\top}{\partial \Theta} = \frac{\partial v^\top}{\partial \Theta} = \left[\frac{\partial \mathbf{v}^{b\top}}{\partial \Theta}, \frac{\partial \boldsymbol{\omega}^{b\top}}{\partial \Theta}, 0_{3\times 1}\right] = \begin{bmatrix} -G^\top S(\mathbf{v}^b) & \dot{G}^\top - G^\top S(\boldsymbol{\omega}^b) & 0_{3\times 1}\end{bmatrix}.$$

The term $\frac{\partial T}{\partial w_i}$ can be expressed as

$$\frac{\partial T_{NU}}{\partial w_i} = \frac{1}{2}\,\dot{q}^\top \mathscr{P}^\top \frac{\partial M_{NU}}{\partial w_i}\mathscr{P}\,\dot{q}$$

with

$$\frac{\partial}{\partial w_i} M_{v\omega} = -\rho A_v S\left(R_z(\alpha_i)\mathbf{r}^b(\varsigma_{pi}) - R_z(\alpha_i)\mathbf{r}^b(-\varsigma_{si})\right)$$

$$\frac{\partial}{\partial w_i} M_{\omega} = -\rho A_v \left(S\left(R_z(\alpha_i)\mathbf{r}^b(\varsigma_{pi})\right)^2 - S\left(R_z(\alpha_i)\mathbf{r}^b(-\varsigma_{si})\right)^2\right)$$

$$\frac{\partial}{\partial w_i} M_{vq}[\,:, i] = \rho A_v \left(R_z(\alpha_i)\frac{\mathrm{d}\mathbf{r}^b}{\mathrm{d}\sigma}(\varsigma_{pi}) - R_z(\alpha_i)\frac{\mathrm{d}\mathbf{r}^b}{\mathrm{d}\sigma}(-\varsigma_{si})\right)$$

$$\frac{\partial}{\partial w_i} M_{vq}[\,:, j \neq i] = 0_{3\times 1}$$

$$\frac{\partial}{\partial w_i} M_{\omega q}[\,:, i] = \rho A_v \left(S\left(R_z(\alpha_i)\mathbf{r}^b(\varsigma_{pi})\right)R_z(\alpha_i)\frac{\mathrm{d}\mathbf{r}^b}{\mathrm{d}\sigma}(\varsigma_{pi}) - S\left(R_z(\alpha_i)\mathbf{r}^b(-\varsigma_{si})\right)R_z(\alpha_i)\frac{\mathrm{d}\mathbf{r}^b}{\mathrm{d}\sigma}(-\varsigma_{si})\right)$$

$$\frac{\partial}{\partial w_i} M_{\omega q}[\,:, j \neq i] = 0_{3\times 1}$$

$$\frac{\partial}{\partial w_i} M_q = 0_{nc\times nc}.$$

According to (5), and (B.2), $\frac{\partial V_{NU}}{\partial q}$ is given by

$$\frac{\partial V_{NU}}{\partial x^n} = \begin{bmatrix} 0 \\ 0 \\ -gm_t \end{bmatrix} = -gm_t\mathbf{z}$$

$$\frac{\partial V_{NU}}{\partial \Theta} = -g\rho \frac{\partial \mathbf{z}^\top R}{\partial \Theta}\left(\sum_{i=1}^{nc}\int_{-\varsigma_{si}}^{\varsigma_{pi}} A_t(\sigma) R_z(\alpha_i)\mathbf{r}^b(\sigma)\mathrm{d}\sigma\right)$$

$$= g\rho G^{\top} S\left(R^{\top}\mathbf{z}\right)\left(\sum_{i=1}^{nc}\int_{-\varsigma_{si}}^{\varsigma_{pi}} A_t(\sigma)R_z(\alpha_i)\mathbf{r}^b(\sigma)\mathrm{d}\sigma\right)$$

$$= g\rho G^{\top} S\left(R^{\top}\mathbf{z}\right)\left(A_h\sum_{i=1}^{nc}\begin{bmatrix}\nu L_h w_i \sin\alpha_i\\ -\nu L_h w_i\cos\alpha_i\\ \nu\left(2L_v e - L_v^2 - w_i^2\right) + L_h e\end{bmatrix}\right)$$

$$\frac{\partial V_{NU}}{\partial w_i} = -g\rho A_v \mathbf{z}^{\top} R(\Theta)\, R_z(\alpha_i)\left(\mathbf{r}^b\left(\varsigma_{pi}\right) - \mathbf{r}^b(-\varsigma_{si})\right).$$

According to (5), V_{NU} is not a function of $\dot{q}$; thus,

$$\frac{\mathrm{d}}{\mathrm{d}t}\frac{\partial V_{NU}}{\partial \dot{q}} = 0_{6+nc\times 1}.$$

We also have

$$\frac{\mathrm{d}}{\mathrm{d}t}\left(\frac{\partial T_{NU}}{\partial \dot{q}}\right)^{\top} = \mathscr{M}_{NU}\,\ddot{q} + \left(\dot{\mathscr{P}}^{\top} M_{NU}\mathscr{P} + \mathscr{P}^{\top}\sum_{i=1}^{nc}\dot{w}_i\frac{\partial M_{NU}}{\partial w_i}\mathscr{P} + \mathscr{P}^{\top}M_{NU}\dot{\mathscr{P}}\right)\dot{q}.$$

Appendix B.3. Summary of NU system dynamics

We write the dynamics of the system as

$$\mathscr{M}_{NU}(q)\,\ddot{q} + C_{NU}(q,\dot{q})\dot{q} + k_{NU}(q) = Q_{hydro}(t,\beta) + Q_{res_{NU}}(\dot{w})$$

with $\mathscr{M}_{NU}(q)$ defined in (A.1), and

$$C_{NU} \triangleq \dot{\mathscr{P}}^{\top} M_{NU}\mathscr{P} + \mathscr{P}^{\top}\sum_{i=1}^{nc}\dot{w}_i\frac{\partial M_{NU}}{\partial w_i}\mathscr{P} + \mathscr{P}^{\top}M_{NU}\dot{\mathscr{P}} - \begin{bmatrix} 0_{3\times 6+nc}\\ \dfrac{\partial(\mathscr{P}\dot{q})^{\top}}{\partial\Theta}M_{NU}\mathscr{P}\\ \dfrac{1}{2}\dot{q}^{\top}\mathscr{P}^{\top}\dfrac{\partial M_{NU}}{\partial w_1}\mathscr{P}\\ \vdots\\ \dfrac{1}{2}\,\dot{q}^{\top}\mathscr{P}^{\top}\dfrac{\partial M_{NU}}{\partial w_{nc}}\mathscr{P}\end{bmatrix}$$

$$k_{NU} \triangleq -g\begin{bmatrix} m_t\mathbf{z}\\ -\rho G^{\top}S\left(R^{\top}\mathbf{z}\right)\sum_{i=1}^{nc}\int_{-\varsigma_{si}}^{\varsigma_{pi}}A_t(\sigma)R_z(\alpha_i)\mathbf{r}^b(\sigma)\mathrm{d}\sigma\\ \rho A_v\mathbf{z}^{\top}R(\Theta)\,R_z(\alpha_1)\left(\mathbf{r}^b\left(\varsigma_{p1}\right) - \mathbf{r}^b(-\varsigma_{s1})\right)\\ \vdots\\ \rho A_v\mathbf{z}^{\top}R(\Theta)\,R_z(\alpha_{nc})\left(\mathbf{r}^b\left(\varsigma_{pnc}\right) - \mathbf{r}^b(-\varsigma_{snc})\right)\end{bmatrix}$$

$$Q_{res_{NU}} = \begin{bmatrix}0_{1\times 6}\\ P_{h_{NU}}^{\top}F_h(\dot{w})\end{bmatrix}$$

$$P_{h_{NU}} = \nu\mathbb{I}_{nc}.$$

Appendix B.4. Summary of *NS* system dynamics

Using the expressions of the energies obtained in Appendix A.2, and following the method used in Appendix B for the *NU* system, we write the dynamics of the *NS* system as

$$\mathscr{M}_{NS}(q)\,\ddot{q} + C_{NS}(q,\dot{q})\dot{q} + k_{NS}(q) = Q_{hydro}(t,\beta) + Q_{res_{NS}}(\dot{w})$$

with

$$\mathscr{M}_{NS}(q) \triangleq \mathscr{P}(\Theta)^{\top}M_{NS}(w)\mathscr{P}(\Theta)$$

$$C_{NS} \triangleq \dot{\mathscr{P}}^{\top} M_{NS} \mathscr{P} + \mathscr{P}^{\top} \sum_{i=1}^{nc} \dot{w}_i \frac{\partial M_{NS}}{\partial w_i} \mathscr{P} + \mathscr{P}^{\top} M_{NS} \dot{\mathscr{P}} - \begin{bmatrix} 0_{3\times 6+nc} \\ \frac{\partial(\mathscr{P}\,\dot{q})^{\top}}{\partial \Theta} M_{NS} \mathscr{P} \\ \frac{1}{2}\,\dot{q}^{\top} \mathscr{P}^{\top} \frac{\partial M_{NS}}{\partial w_1} \mathscr{P} \\ \vdots \\ \frac{1}{2}\,\dot{q}^{\top} \mathscr{P}^{\top} \frac{\partial M_{NS}}{\partial w_{nc}} \mathscr{P} \end{bmatrix}$$

$$k_{NS} \triangleq -g \begin{bmatrix} m_t \mathbf{z} \\ -\rho G^{\top} S(R^{\top}\mathbf{z}) \sum_{i=1}^{N} \int_0^{\varsigma_i} A_t(\sigma) R_z(\alpha_i) \mathbf{r}^b(\sigma) \mathrm{d}\sigma \\ \rho A_v \mathbf{z}^{\top} R(\Theta)\big(R_z(\alpha_1)\mathbf{r}^b(\varsigma_1) - R_z(\alpha_N)\mathbf{r}^b(\varsigma_N)\big) \\ \vdots \\ \rho A_v \mathbf{z}^{\top} R(\Theta)\big(R_z(\alpha_{nc})\mathbf{r}^b(\varsigma_{nc}) - R_z(\alpha_N)\mathbf{r}^b(\varsigma_N)\big) \end{bmatrix}$$

$$Q_{res_{NS}} = \begin{bmatrix} 0_{1\times 6} \\ P_{h_{NS}}^{\top} F_h(\dot{w}) \end{bmatrix}$$

$$P_{h_{NS}} = \nu \begin{bmatrix} \mathbb{I}_{nc} \\ -1_{1\times nc} \end{bmatrix}.$$

Appendix B.5. Summary of *N*P system dynamics

Using the expressions of the energies obtained in Appendix A.3, and following the method used in Appendix B for the *N*U system, we write the dynamics of the *N*P system as

$$\mathscr{M}_{NP}(q)\,\ddot{q} + C_{NP}(q,\dot{q})\dot{q} + k_{NP}(q) = Q_{hydro} + Q_{res_{NP}}(\dot{w})$$

with

$$\mathscr{M}_{NP}(q) \triangleq \mathscr{P}(\Theta)^{\top} M_{NP}(w) \mathscr{P}(\Theta)$$

$$C_{NP} \triangleq \dot{\mathscr{P}}^{\top} M_{NP} \mathscr{P} + \mathscr{P}^{\top} \sum_{i=1}^{nc} \dot{w}_i \frac{\partial M_{NP}}{\partial w_i} \mathscr{P} + \mathscr{P}^{\top} M_{NP} \dot{\mathscr{P}} - \begin{bmatrix} 0_{3\times 6+nc} \\ \frac{\partial(\mathscr{P}\,\dot{q})^{\top}}{\partial \Theta} M_{NP} \mathscr{P} \\ \frac{1}{2}\,\dot{q}^{\top} \mathscr{P}^{\top} \frac{\partial M_{NP}}{\partial w_1} \mathscr{P} \\ \vdots \\ \frac{1}{2}\,\dot{q}^{\top} \mathscr{P}^{\top} \frac{\partial M_{NP}}{\partial w_{nc-1}} \mathscr{P} \\ 0_{1\times 6+nc} \end{bmatrix}$$

$$k_{NP} \triangleq -g \begin{bmatrix} m_t \mathbf{z} \\ -\rho G^{\top} S(R^{\top}\mathbf{z}) \sum_{i=1}^{N} \int_{-\frac{L_h}{2}}^{\varsigma_i} A_t(\sigma) R_z(\alpha_i) \mathbf{r}^b(\sigma) \mathrm{d}\sigma \\ \rho A_v \mathbf{z}^{\top} R(\Theta)\big(R_z(\alpha_1)\mathbf{r}^b(\varsigma_1) - R_z(\alpha_N)\mathbf{r}^b(\varsigma_N)\big) \\ \vdots \\ \rho A_v \mathbf{z}^{\top} R(\Theta)\big(R_z(\alpha_{N-1})\mathbf{r}^b(\varsigma_{N-1}) - R_z(\alpha_N)\mathbf{r}^b(\varsigma_N)\big) \\ 0 \end{bmatrix}$$

$$Q_{res_{NP}} = \begin{bmatrix} 0_{1\times 6} \\ P_{h_{NP}}^{\top} F_h(\dot{w}) \end{bmatrix}$$

$$P_{h_{NP}} = \begin{bmatrix} \nu & 0 & \cdots & 0 & 1 \\ \nu & \ddots & \ddots & \vdots & \vdots \\ \vdots & \ddots & \ddots & 0 & 1 \\ \nu & \cdots & \nu & \nu & 1 \\ 0 & \cdots & 0 & 0 & 1 \end{bmatrix}.$$

References

Chang, C.C., Hsu, C.T., 1998. Control performance of liquid column vibration absorbers. Eng. Struct. 20 (7), 580–586. https://doi.org/10.1016/S0141-0296(97)00062-X.

Christiansen, S., Tabatabaeipour, S.M., Bak, T., Knudsen, T., 2013. Wave disturbance reduction of a floating wind turbine using a reference model-based predictive control. In: American Control Conference (ACC), 2013. IEEE, pp. 2214–2219. https://doi.org/10.1109/ACC.2013.6580164.

Coudurier, C., Lepreux, O., Petit, N., 2015. Passive and semi-active control of an offshore floating wind turbine using a tuned liquid column damper. IFAC-PapersOnLine 48 (16), 241–247. https://doi.org/10.1016/j.ifacol.2015.10.287.

Di Matteo, A., Lo Iacono, F., Navarra, G., Pirrotta, A., 2014. Direct evaluation of the equivalent linear damping for TLCD systems in random vibration for pre-design purposes. Int. J. Non-Linear Mech. 63, 19–30. https://doi.org/10.1016/j.ijnonlinmec.2014.03.009. ISSN 0020-7462.

Ernst, Young, 2015. Offshore Wind in Europe: Walking the Tightrope to success. Technical Report. European Wind Energy Association.

Frahm, H., 1911. Results of trials of the anti-rolling tanks at sea. J. Am. Soc. Nav. Eng. 23 (2), 571–597. https://doi.org/10.1111/j.1559-3584.1911.tb04595.x.

Gao, H., Kwok, K., Samali, B., 1997. Optimization of tuned liquid column dampers. Eng. Struct. 19 (6), 476–486. https://doi.org/10.1016/S0141-0296(96)00099-5. ISSN 0141-0296.

Holden, C., Fossen, T.I., 2012. A nonlinear 7-dof model for U-tanks of arbitrary shape. Ocean. Eng. 45, 22–37. https://doi.org/10.1016/j.oceaneng.2012.02.002.

International Organization for Standardization, 2009. Iso 13624-1-2009 Petroleum and Natural Gas Industries: Drilling and Production Equipment - Part 1: Design and Operation of marine Drilling Riser Equipment.

Jonkman, J.M., 2007. Dynamics Modeling and Loads Analysis of an Offshore Floating Wind Turbine. PhD thesis. National Renewable Energy Laboratory.

Lackner, M.A., Rotea, M.A., 2011. Structural control of floating wind turbines. Mechatronics 21 (4), 704–719. https://doi.org/10.1016/j.mechatronics.2010.11.007.

Landau, L., Lifshitz, E., 1976. Mechanics, third ed. Elsevier.

Larsen, T.J., Hanson, T.D., 2007. A method to avoid negative damped low frequent tower vibrations for a floating, pitch controlled wind turbine. In: Journal of Physics: Conference Series, vol. 75. IOP Publishing. https://doi.org/10.1088/1742-6596/75/1/012073.

Luo, N., Bottasso, C.L., Karimi, H.R., Zapateiro, M., 2011. Semiactive control for floating offshore wind turbines subject to aero-hydro dynamic loads. In: International Conference on Renewable Energies and Power Quality.

Moaleji, R., Greig, A.R., 2007. On the development of ship anti-roll tanks. Ocean. Eng. 34 (1), 103–121. https://doi.org/10.1016/j.oceaneng.2005.12.013. ISSN 0029-8018.

Musial, W., Butterfield, S., Ram, B., et al., 2006. Energy from offshore wind. In: Offshore Technology Conference, pp. 1888–1898. Offshore Technology Conference.

Namik, H., 2012. Individual Blade Pitch and Disturbance Accommodating Control of Floating Offshore Wind Turbines. PhD thesis. ResearchSpace Auckland.

Namik, H., Rotea, M., Lackner, M., 2013. Active structural control with actuator dynamics on a floating wind turbine. In: 51st AIAA Aerospace Sciences Meeting Including the New Horizons Forum and Aerospace Exposition. https://doi.org/10.2514/6.2013-455.

National Renewable Energy Laboratory, 2012. Renewable Energy Data Book. U.S. Department of Energy.

Perez, T., Blanke, M., 2012. Ship roll damping control. Annu. Rev. Control 36 (1), 129–147. https://doi.org/10.1016/j.arcontrol.2012.03.010.

Saeed, T.E., Nikolakopoulos, G., Jonasson, J.-E., Hedlund, H., 2013. A state-of-the-art review of structural control systems. J. Vib. Control. https://doi.org/10.1177/1077546313478294.

Shadman, M., Akbarpour, A., 2012. Utilizing TLCD (tuned liquid column damper) in floating wind turbines. In: ASME 2012 31st International Conference on Ocean, Offshore and Arctic Engineering. American Society of Mechanical Engineers, pp. 241–247. https://doi.org/10.1115/OMAE2012-83330.

Si, Y., Karimi, H.R., Gao, H., 2014. Modelling and optimization of a passive structural control design for a spar-type floating wind turbine. Eng. Struct. 69 (0), 168–182. https://doi.org/10.1016/j.engstruct.2014.03.011. ISSN 0141-0296.

Stewart, G., Lackner, M., 2013. Offshore wind turbine load reduction employing optimal passive tuned mass damping systems. IEEE Trans. control Syst. Technol. 21 (4), 1090–1104. https://doi.org/10.1109/TCST.2013.2260825.

Wu, J.-C., Chang, C.-H., Lin, Y.-Y., 2009. Optimal designs for non-uniform tuned liquid column dampers in horizontal motion. J. Sound Vib. 326 (1–2), 104–122. https://doi.org/10.1016/j.jsv.2009.04.027. ISSN 0022-460X.

Yalla, S., Kareem, A., 2000. Optimum absorber parameters for tuned liquid column dampers. J. Struct. Eng. 126 (8), 906–915. https://doi.org/10.1061/(ASCE)0733-9445(2000)126:8(906).

Yalla, S.K., 2001. Liquid Dampers for Mitigation of Structural Response: Theoretical Development and Experimental Validation. PhD thesis. University of Notre Dame.